Volume 1 | Number 1 | Jan 2013 | Pages 1–100

Materials Horizons

rsc.li/materials-horizons

ROYAL SOCIETY OF CHEMISTRY

ROYAL SOCIETY OF CHEMISTRY

rsc.li/materials-horizons

Conceptual insights

Fluorogens with aggregation induced emission (AIE) characteristics have recently emerged as a new class of fluorescent materials for biosensing and bioimaging applications. AIE fluorogens have shown weak or no fluorescence as molecular species, but intense fluorescence as aggregates. They have attracted considerable attention in the fabrication of molecular fluorescent light-up probes for specific biomarker detection or biological process imaging with high signal-to-background ratios. It is well-known that nanoparticle probes may have distinct advantages over molecular probes, *e.g.*, they can be easily internalized into cells through endocytosis and passively target to tumor tissues *via* enhanced permeability and retention (EPR) effect. However, the bright fluorescence of the AIE aggregates has hampered the development of nanoparticle-based fluorescent light-up probes. In this contribution, by using a simple molecular design strategy, we have developed the first AIE fluorescent light-up nanoparticle probe, which not only possesses tumor-acidity responsiveness with good performance in targeted cancer imaging, but also shows selective inhibition of cancer cells. The smart probe design together with the excellent performance will inspire more exciting research in tumor theranostic platform development, which will further expand the applications of AIE fluorogens in biomedical research.

ARTICLE TYPE

Fluorescent light-up nanoparticle probe with aggregation-induced emission characteristics and tumor-acidity responsiveness for targeted imaging and selective suppression of cancer cells†

Dan Ding,‡[a,b] Ryan T. K. Kwok,‡[c] Youyong Yuan,[a] Guangxue Feng,[a] Ben Zhong Tang*[c,d] and Bin Liu*[a,e]

A pH-responsive light-up nanoparticle probe with aggregation-induced emission (AIE) feature was designed and synthesized. The probe carries negative charges and shows very weak fluorescence in physiological conditions. At tumor acidic extracellular microenvironment, the nanoparticle probe can switch to positive surface charge and thus significantly light up cancer cells, allowing for targeted imaging and selective suppression of cancer cells. As AIE nanoparticles are known for high fluorescence in the aggregate state, this study represents the first example of light-up AIE nanoparticle probe design.

The development of fluorescent light-up bioprobes is of great importance in diagnosis and tracking of many diseases, especially in cancers, as these probes allow sensitive, simple and specific detection of analytes in biological environments.[1] Particularly, designing light-up probes that can response to stimuli in tumor microenvironments would open new avenues to intelligent fluorescent probes for the advancement of cancer imaging. Among the stimuli in tumor microenvironments, pH-responsiveness is of particular interest and it has been extensively investigated in controlled drug delivery for better cancer targeting and treatments.[2] This is because the pH value in tumor extracellular environment (pH_e) is slightly acidic (6.5–7.2) as compared to the blood and normal tissues (~7.4).[3] The enthusiastic researches on pH-triggered drug delivery systems inspired us to explore new pH-responsive fluorescent light-up probes that are capable of imaging cancer cells more intelligently and more efficiently. To date, most of the pH-responsive fluorescent probes are designed for targeting intracellular pH at ~5.5, and only few works have focused on those respond to tumor extracellular acidic microenvironment.[4]

Recently, we have developed a novel class of organic fluorogens with unique aggregation-induced emission (AIE) feature.[5] The AIE fluorogens generally possess rotating units (*e.g.*, phenyl rings). In solution, the low-frequency motions of the rotating units lead to fast non-radiative decay of the excited states, which make the AIE fluorogens non-emissive as molecular species. However, in aggregate state, the intramolecular motion of the rotating units is restricted due to steric hindrance, which opens the radiative pathway, endowing the AIE fluorogens with bright fluorescence.[6] On the basis of the restriction of intramolecular rotation (RIR) mechanism, the AIE fluorogens provide a simple and effective strategy to develop molecular probes that are able to specifically light up upon interaction with biomolecules in solutions and in cells with high signal-to-background ratios.[7] On the other hand, the RIR mechanism limits the applications of AIE fluorogens in the development of nanoparticle-based fluorescent light-up probes, as the confinement of AIE fluorogens in the aggregates leads to high background fluorescence. However, it is well known that nanoparticle probes can be easily internalized into cells through endocytosis.[8] More importantly, as compared to molecular probes, nanoparticle probes can passively target to tumor tissues *via* enhanced permeability and retention (EPR) effect, which enable the probe to achieve longer blood circulation with lower toxicity to normal tissues.[9] Despite the great advantages, it is technically challenging to develop AIE fluorescent light-up nanoparticle probes that can specifically light up in the presence of analytes.
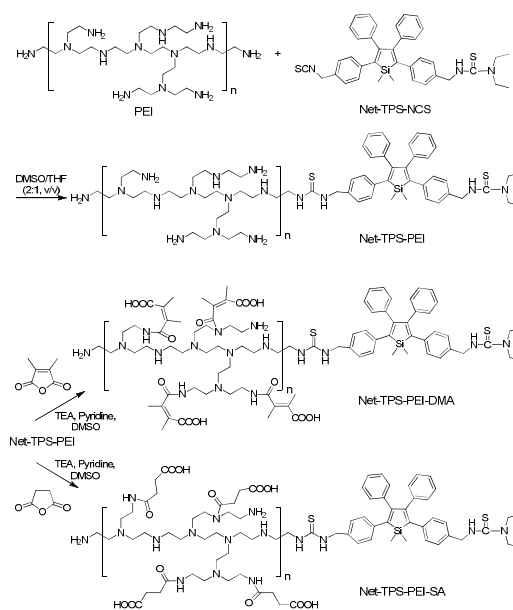
Scheme 1 Synthetic route to nanoparticle probes of Net-TPS-PEI, Net-TPS-PEI-DMA and Net-TPS-PEI-SA.

In this contribution, we report a rational design and synthesis

of a surface charge-switchable light-up nanoparticle probe with AIE signature for targeted imaging and selective suppression of cancer cells. The nanoparticle probe (Net-TPS-PEI-DMA, Scheme 1) is composed of an AIE fluorogen (TPS) and a pH-responsive charge-reversible polymer. Net-TPS-PEI-DMA is negatively charged and nearly non-emissive in physiological conditions (pH = 7.4). Upon exposure to tumor acidic microenvironment (pH_e = 6.5), the surface charge of the nanoparticle probe switches to positive. Electrostatic interactions between positively charged nanoparticle residue and negatively charged cell membrane or cell components not only promote their cellular uptake, but also activate the fluorescence of TPS, achieving targeted cancer cellular imaging in a high contrast and specific manner. The fluorescence of the nanoparticle probes is also observed in tumor tissues *in vivo*. Moreover, it is found that the nanoparticle probe could also suppress the cancer cells. To the best of our knowledge, this is the first report on synthesis and application of AIE fluorescent light-up nanoparticle probes, which will inspire more exciting research in the fields of AIE and bioimaging.
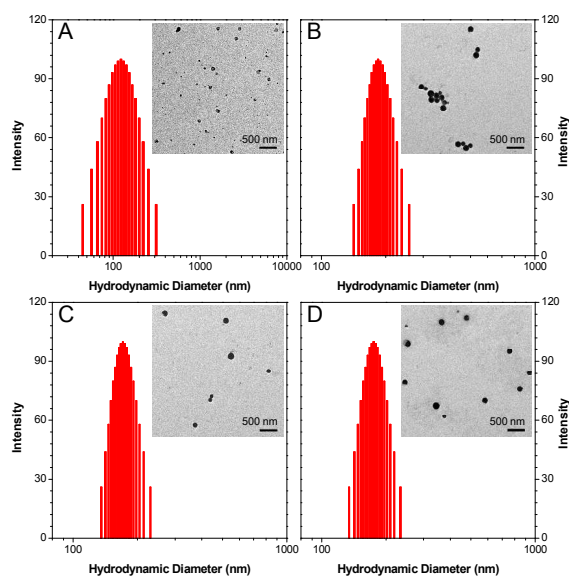
Fig. 1 Hydrodynamic diameter distributions of (A) Net-TPS-NCS, (B) Net-TPS-PEI, (C) Net-TPS-PEI-DMA and (D) Net-TPS-PEI-SA in PBS buffer at pH 7.4. Insets: Transmission electron microscopy (TEM) images of the corresponding nanoparticle probes.
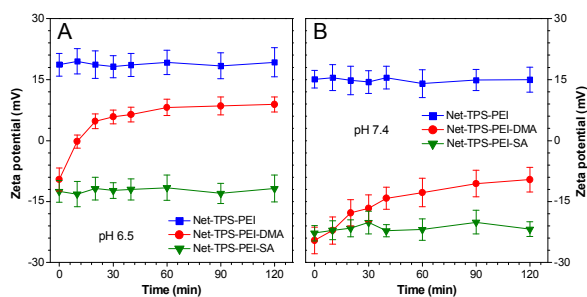
Fig. 2 Zeta potential changes of the nanoparticle probes after incubation in buffers at (A) pH 6.5 and (B) pH 7.4 over time.

3-{4-[5-(4-(Isothiocyanatomethyl)phenyl)-1,1-dimethyl-3,4-diphenyl-silolyl]benzyl}-1,1-diethyl-thiourea (Net-TPS-NCS)

was first synthesized in 63% yield. Detailed synthetic route and characterization (^{1}H and ^{13}C NMR and HRMS spectra) are shown in Scheme S1, Fig. S1 and S2 in ESI†. The Net-TPS-NCS was then conjugated to polyethyleneimine (PEI) to afford Net-TPS-PEI (Scheme 1). The product was characterized by ^{1}H NMR (Fig. S3 in ESI†). It is estimated from the ^{1}H NMR spectrum that ~4.5 of Net-TPS-NCS units were conjugated to one PEI chain on average. Net-TPS-PEI was further reacted with 2,3-dimethylmaleic anhydride (DMA) to convert the residual primary and secondary amines in PEI into amides, yielding Net-TPS-PEI-DMA (Scheme 1). The structure of Net-TPS-PEI-DMA was characterized by ^{1}H NMR (Fig. S4 in ESI†) and there were approximately 660 molecules of DMA on one PEI chain on average. As a control probe, Net-TPS-PEI-SA was also synthesized by replacing DMA with succinic anhydride (SA) to react Net-TPS-PEI using the same reaction conditions as Net-TPS-PEI-DMA. The ^{1}H NMR spectrum of Net-TPS-PEI-SA is shown in Fig. S5 in ESI†. Noteworthy, the amide bonds formed between the primary or secondary amine and DMA are cleavable under tumor acidic microenvironment at pH_e ~6.5 (Fig. S6 in ESI†),[10] while the amide bonds formed between amines and SA cannot be hydrolysed at this pH. Laser light scattering (LLS) results suggest that the average hydrodynamic diameters of Net-TPS-NCS, Net-TPS-PEI, Net-TPS-PEI-DMA and Net-TPS-PEI-SA are approximately 123, 184, 171 and 175 nm, respectively, in phosphate buffered saline (PBS) buffer at pH 7.4 (Fig. 1). Additionally, transmission electron microscopy (TEM) observations indicate that Net-TPS-PEI, Net-TPS-PEI-DMA and Net-TPS-PEI-SA are all well-dispersed and spherical in shape with uniform sizes (inset images in Fig. 1). In comparison, Net-TPS-NCS exhibits a relatively irregular spherical morphology with a smaller size and broader size distribution. These results reveal that all the AIE probes in this study are of nanosize in aqueous media, which are different from the well-established AIE-active molecular probes.[7] The proposed mechanism of Net-TPS-PEI-DMA and Net-TPS-PEI-SA nanoparticle formation is as follows. As Net-TPS-PEI-DMA and Net-TPS-PEI-SA are amphiphilic molecules, the hydrophobic domains of the Net-TPS-PEI-DMA or Net-TPS-PEI-SA molecules tend to be entangled with each other, acting as the interior of the nanoparticles. The negatively charged carboxylic groups of the molecules are exposed to water due to their hydrophilic properties, which serve as the outer layers to stabilize the nanoparticles.

To verify that Net-TPS-PEI-DMA could switch its surface property in response to pH through cleavage of the amide bonds, we investigated the surface zeta potential changes of the nanoparticle probe over time in buffers at pH 6.5 and 7.4. As shown in Fig. 2A, upon incubation of Net-TPS-PEI-DMA in buffer at pH 6.5, the zeta potential of the suspension is negative (-9.6±2.8 mV). The zeta potential increases quickly as the time elapses, which reaches a plateau with a positive zeta potential within 30 min (5.9±1.7 mV). In comparison, Net-TPS-PEI-DMA reveals a constant negative surface charge in buffer at pH 7.4 even after 2 h incubation (Fig. 2B). As control experiments, anionic Net-TPS-PEI-SA and cationic Net-TPS-PEI show negligible change in surface charges in both pH 6.5 and 7.4 buffers over time. These results indicate that acid-responsive cleavage of the amide bonds could only occur in Net-TPS-PEI-

DMA at tumor acidic extracellular microenvironment.

The optical properties of Net-TPS-NCS, Net-TPS-PEI, Net-TPS-PEI-DMA and Net-TPS-PEI-SA nanoprobes incubated in PBS buffer at pH 7.4 and 6.5 for 30 min were studied. All the nanoparticle probes were tested at the same concentration based on 5 μM TPS. As shown in Fig. S7A in ESI†, in PBS buffer at pH 7.4, the Net-TPS-PEI, Net-TPS-PEI-DMA and Net-TPS-PEI-SA nanoparticle probes show similar absorption spectra with a maximum cantered at ~360 nm (similar to the absorption maximum of Net-TPS-NCS in THF), which is blue-shifted as compared to that of Net-TPS-NCS (~375 nm). The difference is due to the Net-TPS-NCS aggregation formation in the aqueous media, while it is relatively well dispersed in the PEI matrices due to the small amount of the dye used for conjugation. Additionally, the absorption spectra of the four nanoparticle probes do not change upon incubation in the buffer at pH 6.5 (Fig. S7B in ESI†). The photoluminescence (PL) spectra of the nanoparticle probes incubated in PBS buffers at pH 7.4 and 6.5 are depicted in Fig. 3A and 3B, respectively. Net-TPS-NCS emits the strongest fluorescence at both pH (with a quantum yield (Φ) of ~18%), whereas the fluorescence intensity of Net-TPS-PEI is around 65% to that of Net-TPS-NCS at both pH. This fluorescence decrement should be due to the highly positive charges of PEI, which reduce the aggregation degree of TPS as compared to the neutral Net-TPS-NCS itself in water. Moreover, Net-TPS-PEI-SA shows slightly different fluorescence intensity as compared to that for Net-TPS-PEI at pH 7.4 and 6.5. Despite of the high surface charges, both Net-TPS-PEI and Net-TPS-PEI-SA show relatively bright fluorescence, they exist as nanoparticles in aqueous media, rather than as molecular species.
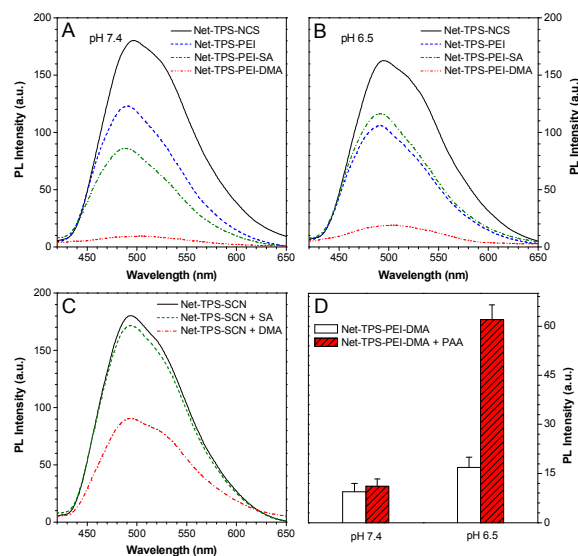
Fig. 3 Photoluminescence (PL) spectra of the nanoparticle probes incubated in PBS buffer at (A) pH 7.4 and (B) pH 6.5 for 30 min. (C) PL spectra of Net-TPS-NCS in PBS buffer upon direct addition of sodium hydroxide solution of DMA or SA. (D) PL intensities of Net-TPS-PEI-DMA upon incubation in PBS buffer at pH 7.4 and 6.5 for 30 min, which was followed by addition of anionic poly(acrylic acid) (PAA).

Although Net-TPS-PEI-DMA is in nanosize (~171 nm), it shows much weaker fluorescence than TPS-PEI-SA in PBS buffer at pH 7.4 with a quite low Φ of 0.85% (Fig. 3A). To understand this unique observation, we incubated DMA or SA in

sodium hydroxide solution (pH 8.5) for 12 h to yield the corresponding acids, and the resultant solutions were subsequently added into the Net-TPS-NCS suspension in PBS buffer. As shown in Fig. 3C, the fluorescence intensity of Net-TPS-NCS does not change with addition of the hydrolyzed SA. On the other hand, the Net-TPS-NCS fluorescence is significantly weakened upon addition of the hydrolyzed DMA. As DMA has a similar chemical structure to SA, this result suggests that the C=C in DMA can quench the TPS fluorescence, endowing Net-TPS-PEI-DMA to be a pH-responsive light-up nanoparticle probe. Therefore, the DMA play dual roles in the light-up nanoprobe design: firstly, it responses to acidic environment; secondly, it serves as a quencher to quench the TPS fluorescence *via* an exciton annihilation process associated with the n-π electronic conjugation of the C=C group.[11] Upon incubation of Net-TPS-PEI-DMA in PBS buffer at pH 6.5 for 30 min, the fluorescence of the probe increases by ~1-fold as compared to that at pH 7.4 (Fig. 3B). This result reveals that only the cleavage of amide bonds cannot significantly switch on the nanoparticle fluorescence, as the released C=C groups can still act as a quencher in the system. When anionic molecules, such as poly(acrylic acid) (PAA) was added into Net-TPS-PEI-DMA in PBS buffer at pH 6.5, strong fluorescence was observed (Φ = 6.6%; Fig. 3D). The fluorescence enhancement is because the electrostatic interactions between the positively charged cleavage residues of Net-TPS-PEI-DMA and the negatively charged PAA leads to formation of large aggregates (~360 nm), which restricts the rotations of the phenyl rings in TPS and activate the emission of the probe. On the contrary, addition of PAA into the solution of Net-TPS-PEI-DMA in buffer at pH 7.4 shows almost no fluorescence change.

As cell membranes are generally negatively charged, we hypothesized that the charge-reversal of Net-TPS-PEI-DMA at tumor extracellular acidic microenvironment could not only enhance their internalization by cancer cells, but also turn-on their fluorescence due to the electrostatic interactions between the positively charged residues of Net-TPS-PEI-DMA and negatively charged cancer cell membranes or cell components (Scheme 2).
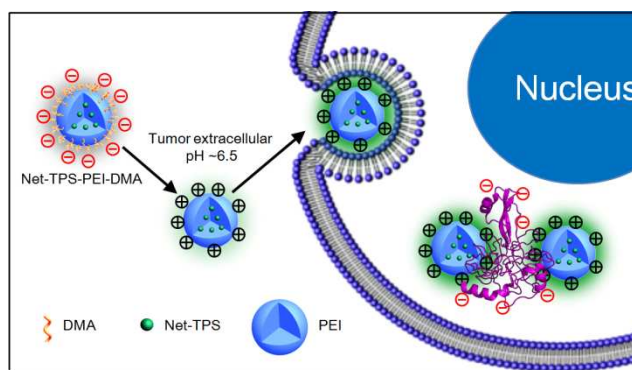
Scheme 2 Schematic illustration of Net-TPS-PEI-DMA as a pH-responsive light-up nanoparticle probe for targeted cancer cell imaging.
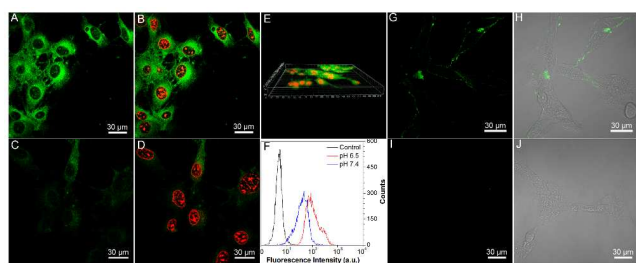
Fig. 4 Confocal laser scanning microscopy (CLSM) images of the MCF-7 cancer cells incubated with Net-TPS-PEI-DMA (green fluorescence) at (A, B) pH 6.5 and (C, D) pH 7.4 for 1 h at 37 °C, respectively. The cell
5 nuclei were stained by PI (red fluorescence) for (B) and (D). (E) 3D confocal image of MCF-7 cancer cells incubated with Net-TPS-PEI-DMA at pH 6.5. (F) Flow cytometry histograms of pure MCF-7 cancer cells and the cells incubated with Net-TPS-PEI-DMA at pH 6.5 and 7.4. CLSM fluorescence and fluorescence/transmission overlay images of
10 MCF-7 cancer cells treated with Net-TPS-PEI-DMA at (G, H) pH 6.5 and (I, J) 7.4 at 4 °C.

To verify our hypothesis, the application of Net-TPS-PEI-DMA for targeted cancer cell imaging was investigated using confocal laser scanning microscopy (CLSM). After incubation
15 with Net-TPS-PEI-DMA (5 μM based on TPS) in the culture medium at pH 6.5 and 7.4 for 1 h at 37 °C, respectively, MCF-7 breast cancer cells were fixed and the cell nuclei were stained with propidium iodide (PI). As shown in Fig. 4A and 4B, intense green fluorescence is observed inside the MCF-7 cancer cells at
20 pH 6.5, while much weaker fluorescence is observed at pH 7.4 (Fig. 4C and 4D). The 3D confocal image of MCF-7 cells incubated with Net-TPS-PEI-DMA at pH 6.5 reveals that the fluorescence is mainly from the cell cytoplasm (Fig. 4E). Additionally, the flow cytometry data indicate that the average
25 fluorescence intensity of each cell incubated with Net-TPS-PEI-DMA at pH 6.5 is ~3.0-fold higher as compared to that at pH 7.4 (Fig. 4F). These results reveal that Net-TPS-PEI-DMA can serve as a light-up nanoparticle probe for targeted cancer cell imaging.

We next treated the MCF-7 cancer cells with Net-TPS-PEI-
30 DMA at 4 °C in culture medium at pH 7.4 and 6.5, respectively. There is obvious green fluorescence distributed on the MCF-7 cell membrane upon incubation at pH 6.5 owing to the electrostatic interaction between cleaved Net-TPS-PEI-DMA residues and cell membrane (Fig. 4G and 4H), whereas almost no
35 visible signal is observed at pH 7.4 (Fig. 4I and 4J). This result further verifies the surface charge switchable as well as light-up properties of Net-TPS-PEI-DMA nanoparticles. Moreover, as the low incubation temperature (4 °C) can suppress energy-dependent endocytosis,[12] the results also suggest that the cleaved Net-TPS-
40 PEI-DMA residues are internalized into cancer cells through endocytosis mechanism.
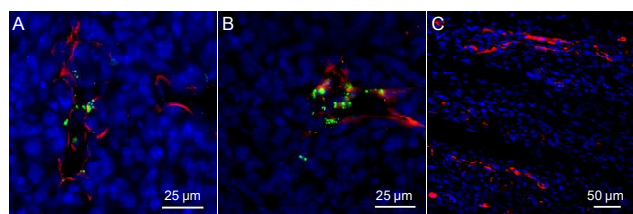
Fig. 5 Representative CLSM images of (A, B) tumor and (C) muscle slices from mice after intravenous injection of Net-TPS-PEI-DMA
45 nanoparticles for (A) 2 h and (B, C) 6 h, respectively. Tumor vasculature was immunostained against platelet/endothelial cell adhesion molecule 1

(PECAM-1; red). The cell nuclei were immunostained against TOPRO-3 (blue).

The application of Net-TPS-PEI-DMA nanoparticle probe in *in*
50 *vivo* tumor imaging was also studied. In this experiment, 4T1 breast cancer cells were subcutaneously inoculated into the right flank of the mice, establishing the tumor-bearing model animals. After intravenous administration of Net-TPS-PEI-DMA nanoparticle probe for 2 h and 6 h, respectively, the mice were
55 sacrificed and the tumor as well as the muscle in mouse leg were sliced for vasculature staining and CLSM imaging. As depicted in Fig. 5A and 5B, the CLSM images from the tumor slices indicates that bright green fluorescent dots from Net-TPS-PEI-DMA nanoparticle aggregation are located close to the tumor
60 blood vessels (red fluorescence) and many are distributed in the tumor cells (blue fluorescence refers to cell nuclei). These results demonstrate that Net-TPS-PEI-DMA nanoparticles can be accumulated in the tumor tissues from blood circulation and turn on their fluorescence at the tumor acidic extracellular
65 microenvironment. In contrast, no fluorescence is detected in the muscle tissues with normal physiological condition (Fig. 5C), demonstrating the nanoparticle fluorescence light-up capability of Net-TPS-PEI-DMA nanoparticle probe in *in vivo* tumor imaging.

The cytotoxicities of the nanoparticle probes against normal as
70 well as cancer cells were investigated after 24 h incubation using a MTT cell-viability assay. As shown in Fig. S8 in ESI†, Net-TPS-PEI shows relatively high cytotoxicity to both normal NIH/3T3 fibroblast cells at pH 7.4 and MCF-7 cancer cells at pH 6.5 at the concentrations of 5, 10 and 20 μM based on TPS. This
75 result is in accordance with the reported cytotoxicity of PEI-based materials, which is ascribed to the highly positive charges of PEI.[13] After conjugation with DMA, the anionic Net-TPS-PEI-DMA shows no obvious cytotoxicity to normal cell lines such as NIH/3T3 fibroblast cells and adipose-derived stem cells at pH 7.4
80 at the concentrations of 5, 10 and 20 μM based on TPS (Fig. 6A). However, when Net-TPS-PEI-DMA incubated at pH 6.5, the probe switches to positively charged, and the resulting probe shows significant cytotoxicity to four different cancer cell lines including MCF-7 breast cancer cells, human hepatocelluar
85 carcinoma cells (HepG2), human cervical cancer cells (HeLa) and human lung cancer cells (NCI-H446) at the tested concentrations (Fig. 6B). These results reveal that Net-TPS-PEI-DMA could be used as a anticancer drug to selectively kill the cancer cells at the tumor acidic extracellular microenvironment.
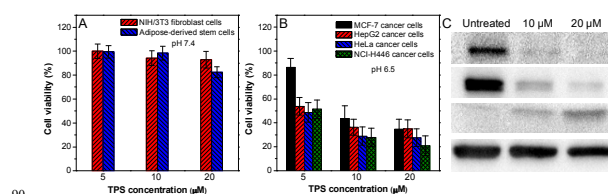
Fig. 6 Metabolic viabilities of (A) two normal cell lines and (B) four cancer cell lines after incubation with Net-TPS-PEI-DMA at pH 7.4 and 6.5 for 24 h, respectively. (C) Western blot analysis of proteins including phosphate-Akt (p-Akt), Bcl-2 and cleaved caspase-3. NCI-H446 cancer
95 cells were treated with Net-TPS-PEI-DMA at pH 6.5 at the concentrations of 10 and 20 μM based on TPS. The structural protein of β-actin was used as a reference, which did not change among samples.

In order to understand the possible mechanism of the anticancer effect of the nanoparticle probes, western blot analysis

was performed upon treatment of NCI-H446 cancer cells with Net-TPS-PEI-DMA at pH 6.5. As shown in Fig. 6C, it is found that the cleaved Net-TPS-PEI-DMA residues suppress the expression of activated form of Akt proteins (phosphate-Akt), down-regulate the expression of Bcl-2 (a protective protein against apoptosis), and induce activation of caspase-3 proteins (a key mediator of cell apoptosis). This result elucidates that the cleaved Net-TPS-PEI-DMA residues result in the cytotoxicity of cancer cells by inhibition of Akt pathway, which triggers the apoptotic cascade.[14]

In summary, we report a light-up nanoparticle probe of Net-TPS-PEI-DMA with AIE feature that responses to tumor acidic extracellular microenvironment. The nanoparticle probe is almost non-fluorescent and carrying negatively charges in physiological conditions. In acidic condition (*i.e.*, pH = 6.5), the surface charges of Net-TPS-PEI-DMA switch to positive, which endow the nanoparticle probe with the abilities to be internalized into the cancer cells as well as significantly turn on its fluorescence. The *in vitro* and *in vivo* experiments demonstrate that Net-TPS-PEI-DMA can significantly light up the cancer cells, which is able to serve as an efficient pH-responsive light-up nanoparticle probe for targeted cancer cell imaging and *in vivo* tumor imaging. The cytotoxicity results also reveal that Net-TPS-PEI-DMA shows low cytotoxicity to normal cells and relatively high cytotoxicity to cancer cells. The high cytotoxicity against cancer cells is also demonstrated to be through the suppression of Akt pathway and activation of apoptotic pathway.

Notes and references

a Department of Chemical and Biomolecular Engineering, National University of Singapore, 117576, Singapore. Fax: +65 67791936; Tel: +65 65168049; E-mail: cheliub@nus.edu.sg

b State Key Laboratory of Medicinal Chemical Biology, Key Laboratory of Bioactive Materials, Ministry of Education, and College of Life Sciences, Nankai University, Tianjin, 300071, China.

c Department of Chemistry, Institute for Advanced Study, Division of Biomedical Engineering, Division of Life Science, State Key Laboratory of Molecular Neuroscience and Institute of Molecular Functional Materials, The Hong Kong University of Science and Technology, Clear Water Bay, Kowloon, Hong Kong, China. E-mail: tangbenz@ust.hk

d SCUT–HKUST Joint Research Laboratory, Guangdong Innovative Research Team, State Key Laboratory of Luminescent Materials and Devices, South China University of Technology, Guangzhou, 510640, China.

*e. Institute of Materials Research and Engineering (A*STAR), 3 Research link, Singapore 117602*

† Electronic Supplementary Information (ESI) available: See DOI: 10.1039/b000000x/

‡ Both authors contributed equally to this work.

1   M. D. Shults and B. Imperiali, *J. Am. Chem. Soc.*, 2003, **125**, 14248; H. Kobayashi, M. Ogawa, R. Alford, P. L. Choyke and Y. Urano, *Chem. Rev.*, 2010, **110**, 2620; I. C. Sun, D. K. Eun, H. Koo, C. Y. Ko, H. S. Kim, D. K. Yi, K. Choi, I. C. Kwon, K. Kim and C. H. Ahn, *Angew. Chem. Int. Ed.*, 2011, **50**, 9348; Y. D. Zhuang, P. Y. Chiang, C. W. Wang and K. T. Tan, *Angew. Chem. Int. Ed.*, 2013, **52**, 8124; H. M. Wang, J. Liu, A. T. Han, N. N. Xiao, Z. S. Xue, G. Wang, J. F. Long, D. L. Kong, B. Liu, Z. M. Yang and D. Ding, *ACS Nano*, 2014, **8**, 1475.

2   D. Schmaljohann, *Adv. Drug Deliv. Rev.*, 2006, **58**, 1655; Y. Y. Yuan, C. Q. Mao, X. J. Du, J. Z. Du, F. Wang and J. Wang, *Adv. Mater.*, 2012, **24**, 5476; M. Kamimura, J. O. Kim, A. V. Kabanov, T. K. Bronich and Y. Nagasaki, *J. Control. Release*, 2012, **160**, 486; W. She, N. Li, K. Luo, C. Guo, G. Wang, Y. Geng and Z. Gu, *Biomaterials*, 2013, **34**, 2252.

3   L. Gerweck and K. Seetharaman, *Cancer Res.*, 1996, **56**, 1194; R. A. Cardone, V. Casavola and S. J. Reshkin, *Nat. Rev. Cancer*, 2005, **5**, 786.

4   Y. Wu, W. Zhang, J. Li and Y. Zhang, *Am. J. Nucl. Med. Mol. Imaging*, 2013, **3**, 1; Y. Zhao, T. Ji, H. Wang, S. Li, Y. Zhao and G. Nie, *J. Control. Release*, 2014, **177**, 11; Y. Y. Yuan, D. Ding, K. Li, J. Liu and B. Liu. *Small*, 2014, **10**, 1967.

5   J. D. Luo, Z. L. Xie, J. W. Y. Lam, L. Cheng, H. Y. Chen, C. F. Qiu, H. S. Kwok, X. W. Zhan, Y. Q. Liu, D. B. Zhu and B. Z. Tang, *Chem. Commun.*, 2001, 1740; Y. N. Hong, J. W. Y. Lam and B. Z. Tang, *Chem. Commun.*, 2009, 4332; Y. N. Hong, J. W. Y. Lam and B. Z. Tang, *Chem. Soc. Rev.*, 2011, **40**, 5361; D. Ding, K. Li, B. Liu and B. Z. Tang, *Acc. Chem. Res.*, 2013, **46**, 2441.

6   M. Wang, G. X. Zhang, D. Q. Zhang, D. B. Zhu and B. Z. Tang, *J. Mater. Chem.*, 2010, **20**, 1858; D. Ding, C. C. Goh, G. X. Feng, Z. J. Zhao, J. Liu, R. R. Liu, N. Tomczak, J. L. Geng, B. Z. Tang, L. G. Ng and B. Liu, *Adv. Mater.*, 2013, **25**, 6083; K. Li, B. Liu, *Chem. Soc. Rev.*, 2014, **43**, 6570. X. Q. Zhang, Z. G. Chi, Y. Zhang, S. W. Liu and J. R. Xu, *J. Mater. Chem. C*, 2013, **1**, 3376; Z. G. Chi, X. Q. Zhang, B. J. Xu, X. Zhou, C. P. Ma, Y. Zhang, S. W. Liu and J. R. Xu, *Chem. Soc. Rev.*, 2012, **41**, 3878.

7   H. B. Shi, J. Z. Liu, J. L. Geng, B. Z. Tang and B. Liu, *J. Am. Chem. Soc.*, 2012, **134**, 9569; H. B. Shi, R. Kowk, J. Z. Liu, B. G. Xing, B. Z. Tang and B. Liu. *J. Am. Chem. Soc.*, 2012, **134**, 17972; Y. Y. Yuan, R. Kwok, B. Z. Tang and B. Liu. *J. Am. Chem. Soc.*, 2014, **136**, 2546; Y. Y. Huang, F. Hu, R. Zhao, G. X. Zhang, H. Yang and D. Q. Zhang, *Chem.-Eur. J.*, 2014, **20**, 158; D. Ding, D. Liang, R. T. K. Kwok, M. Gao, G. X. Feng, Y. Y. Yuan, B. Z, Tang and B. Liu, *J. Mater. Chem. B*, 2014, **2**, 231; X. J. Wang, H. Liu, J. W. Li, K. G. Ding, Z. L. Lv, Y. G. Yang, H. Chen and X. M. Li, *Chem.-Asian J.*, 2014, **9**, 784; X. Q. Zhang, X. Y. Zhang, L. Tao, Z. G. Chi, J. R. Xu and Y. Wei, *J. Mater. Chem. B*, 2014, **2**, 4398.

8   W. Jiang, B. Y. S. Kim, J. T. Rutka, W. C. W. Chan, *Nat. Nanotechnol.*, 2008, **3**, 145.

9   O. C. Farokhzad and R. Langer, *ACS Nano*, 2009, **3**, 16.

10 P. S. Xu, E. A. Van Kirk, Y. H. Zhan, W. J. Murdoch, M. Radosz and Y. Q. Shen, *Angew. Chem. Int. Ed.*, 2007, **46**, 4999; Z. X. Zhou, Y. Q. Shen, J. B. Tang, M. H. Fan, E. A. Van Kirk, W. J. Murdoch and M. Radosz, *Adv. Funct. Mater.*, 2009, **19**, 3580; J. Z. Du, X. J. Du, C. Q. Mao and J. Wang, *J. Am. Chem. Soc.*, 2011, **133**, 17560.

11 Y. Liu, Y. Yu, J. W. Y. Lam, Y. Hong, M. Faisal, W. Z. Yuan and B. Z. Tang, *Chem.-Eur. J.*, 2010, **16**, 8433.

12 P. Watson, A. T. Jones and D. J. Stephens, *Adv. Drug Delivery Rev.*, 2005, **57**, 43.

13 S. M. Moghimi, P. Symonds, J. C. Murray, A. C. Hunter, G. Debska and A. Szewczyk, *Mol. Ther.*, 2005, **11**, 990; S. Werth, B. Urban-Klein, L. Dai, S. Höbel, M. Grzelinski, U. Bakowsky, F. Czubayko and A. Aigner, *J. Control. Release*, 2006, **112**, 257.

14 X. Li, X. Lu, H. Xu, Z. Zhu, H. Yin, X. Qian, R. Li, X. Jiang and B. Liu, *Mol. Pharmaceutics*, 2012, **9**, 222; Y. F. Wang, C. Y. Chen, S. F. Chung, Y. H. Chiou and H. R. Lo, *Cancer Chemother. Pharmacol.*, 2004, **54**, 322.

TOC:
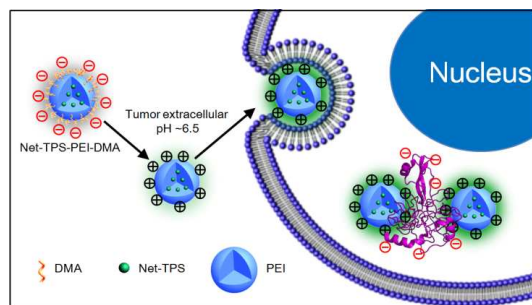
The first pH-responsive light-up AIE nanoparticle probe was designed and synthesized for targeted imaging and selective suppression of cancer cells.